

ORIGINAL
RESEARCH

P.H. Tang
A.I. Bartha
M.E. Norton
A.J. Barkovich
E.H. Sherr
O.A. Glenn



Agenesis of the Corpus Callosum: An MR Imaging Analysis of Associated Abnormalities in the Fetus

BACKGROUND AND PURPOSE: Anomalies associated with callosal agenesis (ACC) found postnatally have been well documented. However, to our knowledge, no detailed MR imaging analysis of associated anomalies has been reported in a large cohort of fetuses with ACC. This study will assess those anomalies and compare them with postnatal cohorts of ACC, to identify associated fetal brain abnormalities that may give insight into etiology and outcome.

MATERIALS AND METHODS: All cases of ACC diagnosed on fetal MR imaging during an 11-year period were retrospectively reviewed, including fetal MR imaging, postnatal MR imaging, and autopsy findings. Neurodevelopmental outcome was classified as poor in children with seizures and/or severe neurodevelopmental impairment or in cases of neonatal death.

RESULTS: Twenty-nine cases of ACC were identified. Median gestational age was 26.14 weeks (range, 19.71–36.43 weeks). Twenty-three fetuses had delayed sulcation and/or too-numerous cortical infoldings (abnormal morphology). Fifteen fetuses had cerebellar and/or brain stem abnormalities. Fetal MR imaging findings suggested a genetic syndrome in 5 fetuses and an acquired etiology or genetic/metabolic disorder in 2 fetuses. Findings were confirmed in 8 cases with postnatal MR imaging, except for delayed sulcation and small vermis, and in 4 cases with autopsy, except for periventricular nodular heterotopia and abnormalities in areas not examined by autopsy. Neurodevelopmental outcome was good in 7 and poor in 9 children. Abnormal sulcal morphology and/or infratentorial abnormalities were present in those with poor outcome and absent in those with good outcome.

CONCLUSIONS: ACC is infrequently isolated in fetuses. Abnormal sulcation is common and suggests more diffuse white matter dysgenesis in these fetuses.

The corpus callosum is the largest commissure connecting the cerebral hemispheres. It develops from the lamina unions of His between 8 and 20 weeks.^{1,2} New insights into the formation of the corpus callosum have identified molecules secreted by midline glial populations that are involved in attracting and repelling axons so that they cross the midline and form the corpus callosum.³ Thus, formation of the corpus callosum is complex; this characteristic may explain why most cases of callosal agenesis (ACC) are not isolated.

ACC can be detected prenatally by routine sonography, for which the important signs include absence of the cavum septum pellucidum, colpocephaly, high-riding third ventricle, and widening of the interhemispheric fissure. Fetal MR imaging is clinically helpful in suspected cases of ACC because it can confirm that the callosum is absent. Moreover, additional abnormalities occur frequently with ACC and are best detected by fetal MR imaging.⁴⁻¹⁰ Although the prognostic implications of prenatally detected ACC are not fully understood, evidence suggests that the presence of additional brain abnormalities imparts a worse prognosis.^{6-8,11-15} We chose to review our experience with cases of ACC and compare them with postnatal cohorts with ACC, to identify associated fetal

brain abnormalities that may give insight into the etiology and outcome.

Materials and Methods

We identified all cases of complete ACC diagnosed by fetal MR imaging performed at our institution between November 1996 and October 2007. All fetal MR imaging examinations were performed on a 1.5T magnet (GE Healthcare, Milwaukee, Wis) using a torso phased-array coil. All fetal MR imaging was performed without maternal or fetal sedation. Single-shot fast spin-echo T2-weighted images were acquired in the axial, sagittal, and coronal planes. In 24 cases, single-shot fast spin-echo T2-weighted images were acquired by using a new technique known as real-time imaging for the fetus, which allows the technologist to interactively control imaging parameters such as slice position, orientation, FOV, and thickness.¹⁶ All images were 3-mm thick with no skip, though in 1 case, the axial images were 4 mm thick, and in 1 case, the sagittal images were 5 mm thick. FOV ranged from 20 to 28 cm depending on gestational age. Whenever possible, imaging was repeated until at least 2 adequate axial, coronal, and sagittal sets of images were obtained, in order to decrease the effect of fetal motion on the study. Nineteen patients also had 5-mm axial fast multiplanar spoiled gradient-recalled T1-weighted images. MR images were retrospectively reviewed by 2 pediatric neuroradiologists who were blinded to the sonographic findings and clinical information. All patients had good- ($n = 25$) or fair- ($n = 4$) quality images; no patient had poor-quality images with severe fetal motion or poor signal intensity to noise.

The following structures were assessed on the fetal MR imaging and scored as normal, abnormal, or suspicious: sulcation pattern and developing cortex; morphology of the ventricles; supratentorial parenchymal signal intensity; supratentorial multilayered pattern; morphology and signal intensity of the deep gray nuclei; morphology of the ventricular walls; and morphology of the brain stem, cerebellum,

Received May 9, 2008; accepted after revision August 22.

From the Departments of Radiology (P.H.T., A.J.B., E.H.S., O.A.G.) and Neurology (A.I.B., E.H.S.), University of California, San Francisco, San Francisco, Calif; Department of Diagnostic Imaging (P.H.T.), KK Women's and Children's Hospital, Singapore; and Kaiser Permanente (M.E.N.), San Francisco, Calif.

Please address correspondence to Orit A. Glenn, MD, UCSF Department of Radiology, Neuroradiology Section, 505 Parnassus Ave, Box 0628, San Francisco, CA 94143-0628; e-mail: Orit.Glenn@radiology.ucsf.edu

 indicates article with supplemental on-line table.

DOI 10.3174/ajnr.A1331

and vermis. A finding was considered suspicious if it was only visualized in 1 plane and could not be confirmed in another plane. Ventriculomegaly was not considered an additional finding because dilation of the posterior lateral ventricles can be attributed to ACC. Sulcation delay was assessed on the basis of published studies.^{17,18} Primary sulci were identified, and each fetus was assigned a sulcation score on the basis of the number of primary sulci present with a maximum score of 34 (17 sulci on each side).

A sulcation score was assigned in a similar manner to 37 control fetuses on the basis of review of their fetal MR images (median gestational age by last menstrual period, 22.71 weeks; range, 21–34 weeks). All control fetuses had normal fetal MR imaging findings and underwent fetal MR imaging for family history of neurologic abnormalities ($n = 22$); as volunteers recruited from sonography and/or obstetrics clinics ($n = 8$); for a maternal history of cerebellar arteriovenous malformation and hemorrhage ($n = 1$); or for suspected abnormality on sonography, including dilated bowel ($n = 1$), prominent posterior fossa fluid ($n = 2$), questionable small vermis on 17-week sonography with a normal vermis seen on 19-week sonography ($n = 2$), questionable prominent midline fluid collection ($n = 1$), a prominent choroid plexus ($n = 1$), and possible small head size on initial sonography, with normal head size on follow-up sonography ($n = 1$).

A logistic function was fitted by nonlinear least squares with the sulcation score as the outcome and gestational age by last menstrual period (LMP) and disease status (control versus ACC) as covariates.¹⁹ Thirteen patients had repeated measurements in the dataset. These were modeled as independent observations because there was not enough repeated data to support a longitudinal model. The fitted logistic curve for controls was compared against the curve for patients with ACC by using χ^2 likelihood ratio testing. In addition, comparisons of proportions of fetal brain abnormalities were performed by using the 2-sided Fisher exact test. Suspicious findings were coded as normal for the statistical analyses. Because of the exploratory nature of our comparisons, we report uncorrected P values with emphasis on $P < .05$.

Sonographic reports were available for all cases and were reviewed to identify the suggested sonographic diagnosis before fetal MR imaging. When patients underwent a second fetal MR imaging during the pregnancy, images were also reviewed and assessed in a manner similar to that used to review the first fetal MR imaging. Postnatal MR images, when available, were reviewed and assessed in a manner similar to that of the fetal MR imaging, and the findings were compared. Postnatal MR imaging was performed at different institutions; and images included axial, coronal, or sagittal 3D spoiled gradient-recalled T1-weighted images (1.5-mm thickness, no skip) and/or 3D coronal fast spin-echo T2-weighted images (1.5-mm thickness, no skip) in all patients except 1; axial spin-echo T2-weighted images in all patients (4- to 6-mm section thickness, 0.5- to 2-mm skip); sagittal spin-echo T1-weighted images (3- to 5-mm thickness; skip, 1 mm) in 5; and axial spin-echo T1-weighted images (4- to 5-mm thickness; skip, 1–1.5 mm) in 3. Autopsy reports of the fetal brain were also reviewed when available and compared with fetal MR imaging findings.

Neurodevelopmental outcome was assessed by a postnatal questionnaire administered to the parents (for living children), which included questions about attainment of neurodevelopmental milestones, presence of seizures, hospitalizations, and need for therapeutic interventions, and by review of medical records (for both living children and cases of neonatal death). Living children who had no seizures, motor, or cognitive impairment were classified as having

a good neurodevelopmental outcome. Neonatal deaths or children with seizures, motor, and/or cognitive impairment were classified as having a poor neurodevelopmental outcome. Five cases have been previously published.⁵

This study was approved by our institutional review board.

Results

Twenty-nine cases of ACC were diagnosed on fetal MR imaging during an 11-year period. Median gestational age based on LMP was 26.14 weeks (range, 19.71–36.43 weeks). Median gestational age based on sonographic measurements was 26.57 weeks (range, 19.86–37.00 weeks). There was an average interval of 5.38 days between the sonography and fetal MR imaging (range, 0–17 days). Twenty-seven cases were singleton pregnancies, and 2 cases were dichorionic diamniotic twin pregnancies in which 1 twin had ACC. Three fetuses also had a second antenatal MR exam obtained between 6 and 7.43 weeks (mean, 6.48 weeks) after the first fetal MR exam. Twenty-six fetuses were referred for fetal MR imaging for sonographically suggested ACC, 1 fetus was referred for isolated mild ventriculomegaly on sonography, 1 was referred for ventriculomegaly and a small cerebellum, and 1 was referred for a small vermis. Additional findings were detected by sonography in 13 fetuses and included the following: small or absent vermis ($n = 4$), small or absent cerebellum ($n = 4$), irregularity of the ventricular wall suggestive of periventricular nodular heterotopia ($n = 6$), choroid plexus cysts ($n = 3$), abnormal brain stem ($n = 2$), germinal matrix and intraventricular hemorrhage ($n = 1$), and a focal sulcal malformation ($n = 1$).

Fetal MR Imaging Findings

Sulcation abnormalities were present in 23 fetuses (on-line Table). Twelve patients had abnormal sulcal morphology characterized either by abnormal, too numerous infoldings (11 fetuses) or by absent sulcation (1 case). In 3 patients, the abnormal, too numerous cortical infoldings were unilateral, though there was delayed sulcation in the contralateral cerebral hemisphere (Fig 1A). A delay in sulcation was observed in 20 patients, including those with normal sulcal morphology. Interestingly, sulcation delay was detected only in those fetuses that were 29 weeks or younger; those 30 weeks or older did not have sulcal delay.

Abnormal morphology of the lateral ventricle was always seen in association with abnormal sulcal morphology (Fig 2A) and always involved at least the frontal horn, which was either incompletely formed, showed undulations along the margin, and/or was focally dilated (Fig 2B). The abnormality was unilateral in 5 of the 7 cases and occurred on the side with the abnormal cortical infoldings or more severe abnormal cortical infoldings (if both cerebral hemispheres were involved). In 5 fetuses, the atria were also enlarged. A total of 25 fetuses had enlargement of the ventricular atria, with a median size of 13.5 mm (range, 10–68.2 mm).

Abnormal signal intensity in the supratentorial parenchyma was characterized most often by T2 hypointensity underlying areas of abnormal cortical infoldings (Fig 1B) or diffusely in association with lissencephaly. Two patients had heterogeneous signal intensity in the parenchyma with areas of injury, hemorrhage, and/or necrosis (Fig 3). The multilay-

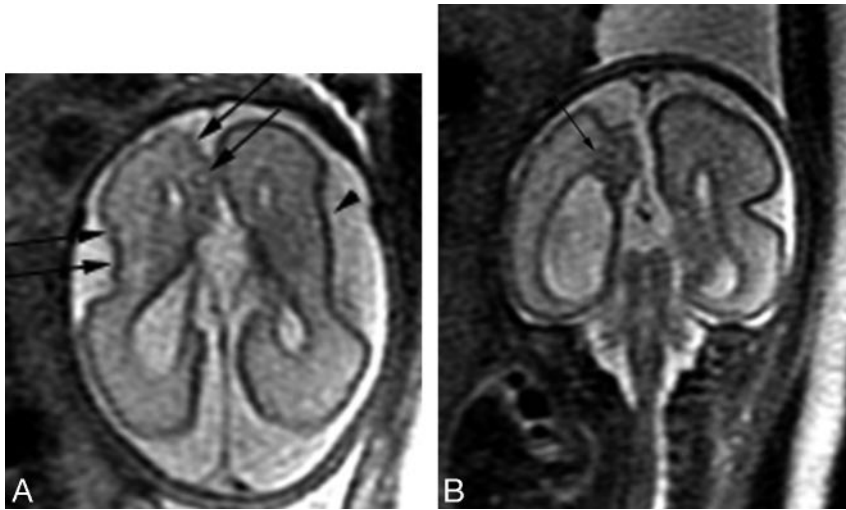


Fig 1. Patient 20: 28.86-gestational-week fetus. A, Axial image demonstrates numerous abnormal cortical infoldings (black arrows) in the right hemisphere with a shallow left Sylvian fissure (arrowhead). B, Coronal image demonstrates an area of hypointensity (arrow) underlying the abnormal cortical infoldings.

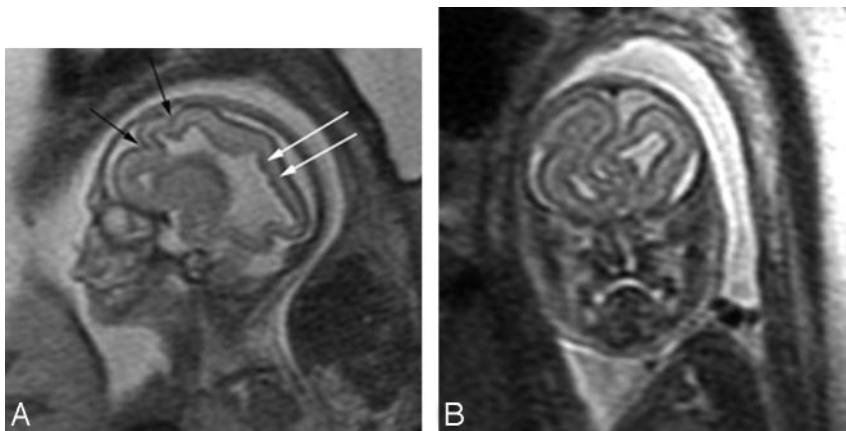


Fig 2. Patient 7: 22-gestational-week fetus. A, Sagittal image demonstrates multiple abnormal infoldings of the cortex (black arrows). The lateral ventricle is dysplastic with multiple undulations along its margin. Periventricular nodular heterotopia are seen (white arrows). The multilayered pattern of the supratentorial parenchyma is absent. B, Coronal image demonstrates abnormal infoldings of both frontal lobes with the left frontal lobe extending across the midline and dilated dysplastic frontal horns bilaterally. A diagnosis of Aicardi syndrome was confirmed postnatally.



Fig 3. Patient 3: 21-gestational-week fetus. Axial image demonstrates areas of hypointensity and hyperintensity involving the deep gray nuclei bilaterally (arrowheads), consistent with areas of hemorrhage and necrosis. There is bilateral ventriculomegaly with diffuse thinning of the parenchyma, with areas of hypointensity in the occipital and parietal lobes (arrows).

ered pattern (which is normally seen between the 20th and 29th gestational weeks) was absent in 9 fetuses and indistinct in 2 (Fig 2A). All had sulcation delay. In 7 fetuses, the affected hemisphere also had abnormal sulcal morphology, whereas 2 also had severe parenchymal destruction.

Three patients had dysplastic-appearing deep gray nuclei characterized by small size and abnormal shape, and all had associated abnormal sulcal morphology and posterior fossa abnormalities (Fig 4). The deep gray nuclei were small, with areas of mixed hypointense and hyperintense T2 signal inten-

sity consistent with hemorrhage and necrosis in 2 fetuses with parenchymal signal-intensity abnormalities, sulcation delay, and posterior fossa abnormalities (Fig 3).

Periventricular nodular heterotopia (PVNH) were present in 4 fetuses (Fig 5). In 5 fetuses, nodularity along the ventricular wall was seen in only 1 plane and thus was considered suspicious. PVNH was usually seen in association with abnormal sulcal morphology, though it was seen only in association with delayed sulcation in 1 fetus and it was the only additional finding in 1 fetus.

Fifteen fetuses had infratentorial brain abnormalities. The cerebellum was abnormal in 13; suspicious in 1 with a small vermis, where the right cerebellum appeared small with abnormal orientation of the folia on 1 axial image; and suspicious in 1, with an asymmetric appearance of the fourth ventricle and right cerebellum appearing small on only 1 axial series. Both cerebellar hemispheres were abnormal in 10 fetuses, and unilateral involvement was seen in 3 (Fig 6A). The cerebellum was small in 7 fetuses, and abnormal morphology was identified in 6, 5 of which were also small. Two of the fetuses with a small cerebellum had evidence of compression of the posterior fossa structures by either a posterior fossa cyst or hydrocephalus. The vermis was absent in 2 fetuses and small in 10 and was usually associated with an abnormal cerebellum and brain stem. The brain stem was abnormal in 10 of the 13 fetuses with an abnormality of the cerebellar hemispheres and in 1 with a normal cerebellum but small vermis (Fig 6B). The

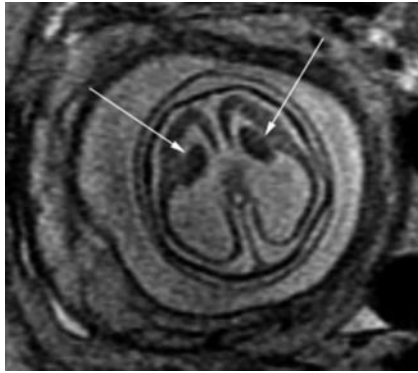


Fig 4. Patient 10: 23-gestational-week fetus. Axial image demonstrates small abnormally shaped deep gray nuclei (arrows). The Sylvian fissures are absent, and there is diffuse thinning and hypointensity of the parenchyma. A diagnosis of Walker-Warburg syndrome was confirmed by autopsy.

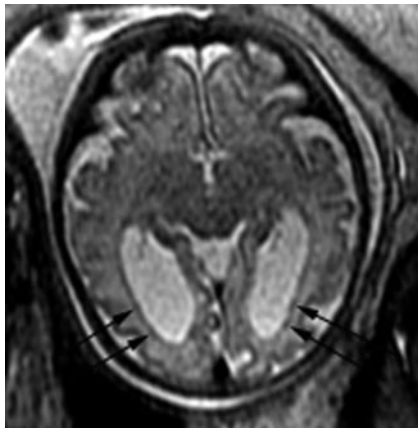


Fig 5. Patient 29: 36.43-gestational-week fetus. Axial image demonstrates bilateral periventricular nodular heterotopia (black arrows) and mild ventriculomegaly.

brain stem appeared dysplastic in 7 fetuses, small in 2 fetuses and was compressed in 2 from either a posterior fossa cyst or marked hydrocephalus.

In 5 fetuses, there were extensive additional malformations identified by fetal MR imaging and suggestive of a genetic syndrome. These included 2 cases of Aicardi syndrome (1 confirmed postnatally); 1 case of Walker-Warburg syndrome (confirmed by autopsy); 1 case of clinically diagnosed oral-facial-digital syndrome (Type I); and 1 case of clinically diagnosed mental retardation, aphasia, shuffling gait, and adducted thumbs (MASA) syndrome (pending genetic testing confirmation of a *LICAM* mutation).

Three patients underwent a second antenatal MR exam. Changes since the first MR imaging included increased mild ventriculomegaly in all 3, more marked dysplasia of the lateral ventricles in 1 case, more numerous abnormal infoldings of the cortex in 1 case, and normalization of sulcation delay in 1 case (Fig 7).

There was a statistically significant delay in sulcation in fetuses with ACC compared with controls ($P < .0001$). The proportion of patients with delayed sulcation was higher in those patients who were younger than 30 weeks gestation than in those patients who were 30 weeks gestation or older ($P = .000007$). The proportion of patients with dysplastic ventricles was higher in those patients with abnormal sulcal morphology

compared with those with normal sulcal morphology ($P = .0009$). The proportion of patients with parenchymal signal-intensity abnormalities was higher in those patients with abnormal deep gray nuclei compared with those with normal deep gray nuclei ($P = .03$). The proportion of patients with abnormal deep gray nuclei was higher in those patients with posterior fossa abnormalities compared with those with a normal posterior fossa ($P = .04$). There was a trend toward a greater proportion of patients with abnormal sulcal morphology in those with posterior fossa abnormalities compared with those with a normal posterior fossa ($P = .054$).

Postnatal Follow-Up, Postnatal MR Imaging, and/or Autopsy Findings

There were 16 live births. Postnatal MR imaging was performed in 8 patients (on-line Table). Postnatal MR imaging was performed between 2 days and 23 months of age. An autopsy was performed in 4 cases (on-line Table) and in 1 case, both a postnatal MR exam and neonatal autopsy were performed. Fetal autopsy was performed 5 days after the fetal MR exam in 1 case. In 3 cases, neonatal death occurred between 1 and 5 days of birth, and a postnatal autopsy was performed (interval between fetal MR exam and autopsy was 2.43 weeks, 3.71 weeks, and 11.28 weeks).

Fetal MR imaging findings were confirmed in all cases with postnatal MR imaging, except for delay in sulcation, which was not present on the postnatal MR images; 1 case of small vermis; and 2 cases of suspected PVNH. In all 3 cases with PVNH on fetal MR imaging, findings were confirmed on postnatal MR imaging. However, in 2 cases with fetal MR imaging findings suspicious for PVNH, there was no evidence of PVNH on postnatal MR imaging. Findings on postnatal MR imaging that were not detected on fetal MR imaging included a dorsal defect in the pons, small foci of white matter injury, germinal matrix hemorrhage, an area of deep cortical infolding consistent with cortical malformation (in a case in which fetal MR imaging was too limited to assess sulcal morphology), and dysplastic deep gray nuclei (in a case in which fetal MR imaging was too limited to assess the deep gray nuclei).

Fetal MR imaging findings were confirmed in nearly all cases with autopsy, except for 1 case of dysplastic deep gray nuclei in which postmortem did not examine the deep gray nuclei, 1 case of destructive/hemorrhagic changes in the posterior parietal and occipital lobes that were not clearly examined on autopsy (the postmortem report only commented on the normal frontal lobes and did not comment on the parietal, occipital, or temporal lobes), and 2 cases of PVNH not mentioned in the postmortem report. Interestingly, in 1 case with both postnatal MR imaging and neonatal autopsy, PVNH was confirmed by postnatal MR imaging but not mentioned on the postmortem report; this discrepancy likely reflects the limitations of autopsy. Neuropathologic findings that were not seen on fetal MR imaging included heterotopia in the cerebellar white matter, ectopic neurons in the subcortical cerebral white matter, small/absent cranial nerves, absent olfactory bulbs, and 1 case of acute intraventricular and left cerebellar hemorrhage in which the new findings could possibly have been related to termination of pregnancy performed after the fetal MR imaging.

Of the 16 live births, 3 neonates died during the neonatal

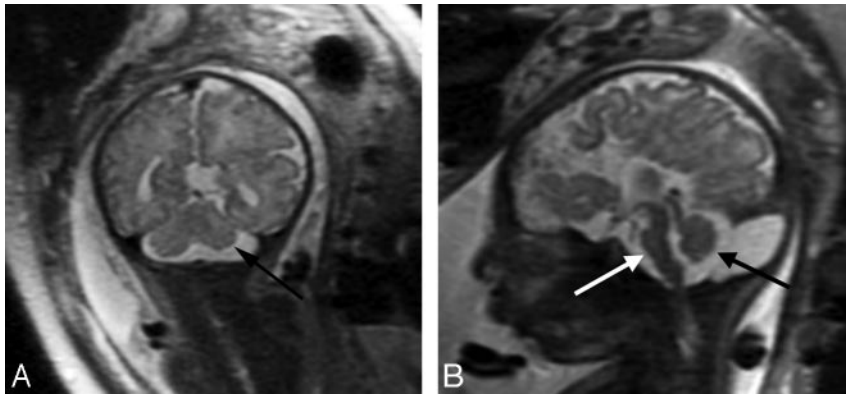


Fig 6. Patient 28: 36-gestational-week fetus. *A*, Coronal image demonstrates a small left cerebellar hemisphere (arrow). The sulcation pattern is also diffusely abnormal with too-numerous infoldings of the cortex bilaterally. *B*, Sagittal image demonstrates a small pons (white arrow) and a small vermis (black arrow) as well as ACC.

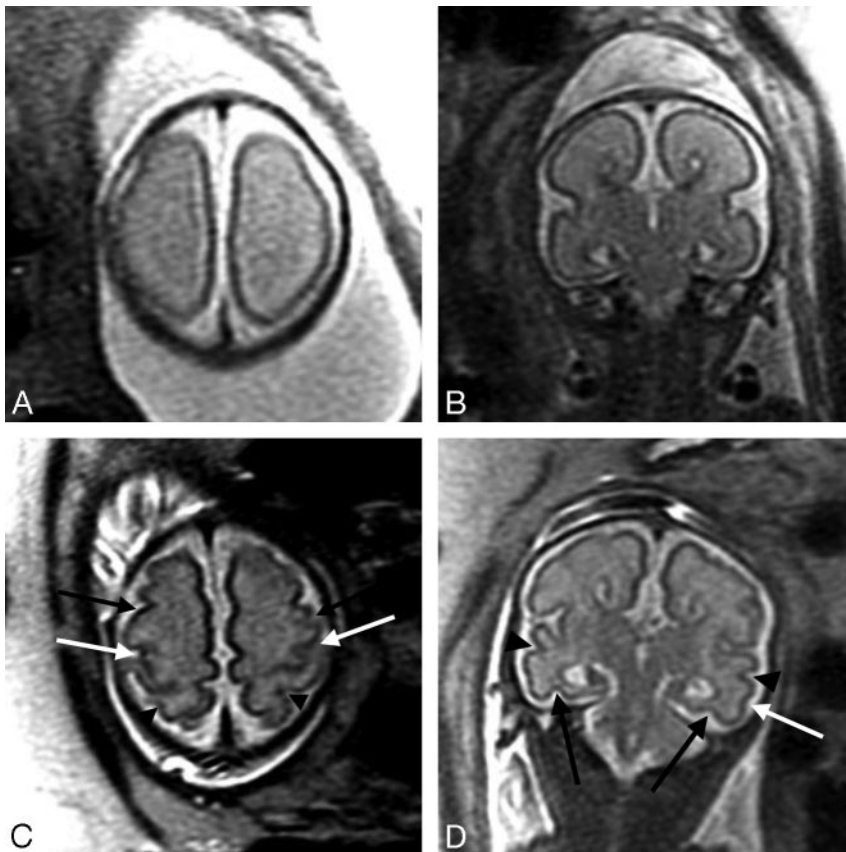


Fig 7. Patient 16: 26.43-gestational-week fetus. *A*, Axial image demonstrates absence of the central sulci, which should be present at this gestational age. *B*, Coronal image demonstrates ACC as well as prominence of the temporal horns (the atria were mildly dilated as well) and absence of the collateral sulci, which should normally be present at this gestational age. *C*, Axial image from follow-up fetal MR imaging performed at 32.43 gestational weeks demonstrates a normal appearance of the sulci for gestational age, including formation of the central sulci bilaterally (white arrows), precentral sulci bilaterally (black arrows), and postcentral sulci bilaterally (arrowheads). *D*, Coronal image at 32.43 gestational weeks demonstrates interval development of the collateral sulci bilaterally (black arrows), superior temporal sulci bilaterally (arrowheads), and inferior temporal sulcus on the left (white arrow).

period, 6 have seizures and/or severe neurodevelopmental disabilities, and 7 are healthy or have only mild neurodevelopmental delays (on-line Table). The causes of neonatal death were prematurity in the setting of Walker-Warburg syndrome, pneumothorax and respiratory failure in the setting of brain stem dysfunction, and respiratory failure and minimal motor function in the setting of brain stem compression from severe hydrocephalus. Of the living patients, 1 has required placement of a ventriculoperitoneal shunt but has done well developmentally. The proportion of patients with abnormal sulcal morphology was higher in those with poor neurodevelopmental outcome compared with those with good neurodevelopmental outcome ($P = .01$). In the patients with poor neurodevelopmental outcome, there was also a higher proportion of cerebellar abnormalities ($P = .003$), vermian abnormalities ($P = .003$), and brain stem abnormalities ($P = .001$), compared with those with good neurodevelopmental out-

come. Among those with good neurodevelopmental outcome, 1 had PVNH, 1 had suspicion for PVNH (not confirmed by postnatal MR imaging), 3 had sulcation delay, and 1 had an indistinct multilayered pattern.

Discussion

We observed additional brain abnormalities in 27/29 of fetuses with ACC. The most common findings were sulcation abnormalities, followed by posterior fossa abnormalities. Abnormal sulcal morphology (12/28) could be detected as early as 19 gestational weeks and was just as frequently detected in fetuses less than 24 gestational weeks as it was in fetuses older than 24 gestational weeks. Abnormal sulcal morphology was nearly always associated with multiple brain abnormalities and was associated with a specific syndrome in 42% of cases. Moreover, abnormal T2 hypointensity was often seen in the parenchyma underlying areas of abnormal sulcal morphology,

suggestive of more extensive dysplasia involving more than just the developing cortex. This is not so dissimilar to what is observed in children with ACC, with gyral malformations being a common additional finding. In a recent study of children with ACC and callosal hypogenesis, Hetts et al²⁰ observed sulcal abnormalities in 51% of children with ACC. The gyral abnormalities included polymicrogyria, lissencephaly, pachygyria, schizencephaly, and other nonclassified abnormalities. Moreover, studies of fetuses with ACC have also shown that gyral abnormalities are among the most common additional malformations seen in ACC either on fetal MR imaging or autopsy.^{4,9}

We also observed a delay in sulcation in many fetuses with ACC. This is particularly interesting because the mechanisms underlying cortical folding are not well understood and are likely complex. Sulcal formation has been postulated by Van Essen²¹ and Toro and Burnod²² to be related to tension exerted on the developing cortex by axonal connections, including intracortical connections, resulting in infolding of the developing cortex; some have postulated that it may be also related to cortical growth.^{22,23} Moreover, the formation of sulci seems to be related to the cytoarchitectural organization of brain.²⁴ Fischl et al²⁴ showed that the cortical folding patterns are less variable in areas of more basic function, such as motor and visual function, compared with areas involved in higher cortical function. They postulated, on the basis of Van Essen's theory that cortical folds form from tensions along axons in the white matter that connect to the cortex,²¹ that areas involved with more connections have more heterogeneity in folds.

Our finding of sulcation delay suggests that there is more global white matter dysgenesis in fetuses with ACC. Indeed, recent studies on children and adults with ACC using diffusion tensor imaging have shown that the fibers that are meant to cross the midline through the corpus callosum instead course in an anterior-to-posterior direction in Probst bundles, forming aberrant connections between axons from within the same hemisphere.²⁵⁻²⁷ Interestingly, the Probst bundles appear to have a dorsal-ventral pattern of organization.^{26,27} On the basis of Van Essen's theory²¹ of cortical folding, it is possible that the absence of normal connections between hemispheres and formation of aberrant connections within the same hemisphere could delay the formation of primary sulci and perhaps even contribute to the abnormal sulcal morphology seen in so many of these fetuses. It is also possible that the observed delay in sulcation may be a result of sulci being shallower in the setting of ventriculomegaly and, therefore, more difficult to detect. Sulcation might also seem delayed because dates could have been unreliable and confirmation of dates by first trimester sonography was not available for most patients. Our observed delay in sulcation compared with that in controls needs to be verified in a larger series, preferably by using more sensitive techniques to study sulcation, such as 3D morphometry.

Interestingly, although sulcation delay was observed in nearly all fetuses younger than 30 gestational weeks, it was not observed in fetuses older than 30 gestational weeks or on postnatal MR imaging. Moreover, 1 fetus had isolated sulcation delay on the first fetal MR exam performed at 26.4 gestational weeks and a normal sulcation pattern on the second fetal MR

exam performed at 32.4 gestational weeks. This finding suggests that though initially delayed, the primary sulci do eventually form. It is possible, however, that there is a more subtle abnormality in the formation of the primary sulci that persists beyond 29 gestational weeks that was not detected by our methods and that might be detected by more sensitive methods, such as 3D morphometry. Moreover, more sensitive methods such as 3D morphometry might be able to detect abnormalities in secondary and tertiary sulcal formation and provide further insight into the formation of sulci in fetuses with ACC. Future studies using diffusion-weighted and diffusion tensor imaging could also give insight into the microstructure of the white matter in areas of delayed sulcation. This would be especially interesting in light of the fact that nonclassified abnormal sulcal morphology is a common finding in children with ACC.²⁰

Posterior fossa abnormalities were also a common additional finding, which has been observed in other studies of prenatally diagnosed ACC with fetal and/or postnatal MR imaging.^{4,10,11,28-30} Interestingly, cerebellar hemispheric abnormalities were more common than vermian abnormalities in our study, a finding that is similar to those in other prenatal MR imaging studies^{4,10} but different from those in postnatal MR imaging studies,^{20,31} perhaps due to the difficulty in evaluating the fetal vermis or due to termination of those cases with prenatally diagnosed cerebellar abnormalities. Brain stem abnormalities were also common, occurring in 33% of patients in our study. All brain stem abnormalities occurred in the setting of an abnormal cerebellum except 1 case in which the brain stem and vermis were small but the cerebellum appeared normal (though actual measurements could not be made due to marked obliquity of the images). Our findings strongly suggest that in the setting of cerebellar abnormality, the brain stem should be carefully evaluated.

In our study, only 7% of cases of ACC were isolated on fetal MR imaging. This is lower than what has been reported in previous studies using fetal MR imaging^{4,5,10,28} and may be due to the younger gestational age and increased number of fetuses in our study. If we exclude sulcation delay, then 69% had additional findings on fetal MR imaging, which is more similar to findings in prior studies of fetal ACC using either fetal MR imaging and/or postnatal imaging.^{4,5,10,11,28,29} In addition, fetal MR imaging identified abnormalities not detected by prenatal sonography in most (83%) patients; this difference is in agreement with prior studies and further supports the need for fetal MR imaging in cases of sonographically suspected ACC.^{5,28,30,32,33}

In most fetuses, the additional abnormalities were suggestive of a developmental etiology. In 5 fetuses (17%), there were extensive additional malformations identified by fetal MR imaging and suggestive of a genetic syndrome. These included 2 cases of Aicardi syndrome (1 confirmed postnatally), 1 case of Walker-Warburg syndrome (confirmed on autopsy), 1 case of clinically diagnosed oral-facial-digital syndrome (Type I), and 1 case of clinically diagnosed MASA syndrome. Interestingly, in 3/29 (10%) fetuses, there was evidence of destructive changes in the brain parenchyma, suggesting either an acquired etiology or genetic/metabolic abnormality, which can be associated with ACC.

Although nearly half of the cases resulted in termination of

pregnancy, we did observe that the presence of additional abnormalities was associated with a poor neurodevelopmental outcome. In particular, abnormal sulcal morphology and/or infratentorial abnormalities were present in all patients with poor neurodevelopmental outcome and absent in all patients with good neurodevelopmental outcome. This is in agreement with findings in prior studies showing that the presence of additional brain abnormalities imparts a worse prognosis.^{6-8,11-15} Interestingly, we did observe sulcation delay in many patients, including those with a good neurodevelopmental outcome, which suggests that the sulcation delay is actually a manifestation of the white matter dysgenesis that likely occurs in ACC, rather than a separate or additional abnormality. Longer term neurodevelopmental studies, however, are needed in these patients because developmental delays have been observed in children with prenatally diagnosed isolated ACC^{7,10,12,34,35} and may not be detected until school age.³⁴

Our study is limited by the fact that fetal MR imaging was performed at many different gestational ages. It is likely that the sensitivity of fetal MR imaging for certain brain abnormalities might increase with increasing gestational age, given the increased head size and decreased fetal motion with increasing gestational age. Thus, performing fetal MR imaging at a consistent gestational age (and perhaps twice during the pregnancy) would probably give a better idea of the accuracy of the study, though it is not clinically practical. Postnatal MR imaging or autopsy was performed in only 38% of the cases, which limits our assessment of the accuracy of fetal MR imaging. In all cases in which a postnatal MR exam was performed, however, we were able to collect and view the images in a blinded manner. Our study is also limited by the short-term follow-up of many of our patients to younger than 2 years of age. Longer follow-up is needed, with more formal neurodevelopmental testing, because behavioral and cognitive difficulties may not be detected until the children reach school age.³⁴

Conclusions

Isolated ACC is infrequent, with sulcal and infratentorial abnormalities as common findings. Sulcation delay was present in most fetuses with ACC, including those with a good neurodevelopmental outcome, and suggests a more global white matter dysgenesis. Future studies using diffusion-weighted and diffusion tensor imaging in the fetus are needed to give insight into the structure of white matter in fetuses with ACC.

References

- Rakic P, Yakovlev P. **Development of the corpus callosum and cavum septi in man.** *J Comp Neurol* 1968;132:45–72
- Barkovich AJ. *Pediatric Neuroimaging*. 4th ed. Philadelphia: Lippincott Williams & Wilkins; 2005
- Shen W, Plachez C, Mongi AS, et al. **Identification of candidate genes at the corticoseptal boundary during development.** *Gene Expr Patterns* 2006;6:471–81. Epub 2006 Feb 2
- Brisse H, Sebag G, Fallet C, et al. **IRM antenatale des agenesies calleuses: etude de 20 cas avec correlations neuropathologiques.** *J Radiol* 1998;79:659–66
- Glenn O, Goldstein RB, Li KC, et al. **Fetal MRI in the evaluation of fetuses**

- referred for sonographically suspected abnormalities of the corpus callosum.** *J Ultrasound Med* 2005;24:791–804
- Goodyear PW, Bannister CM, Russell S, et al. **Outcome in prenatally diagnosed fetal agenesis of the corpus callosum.** *Fetal Diagn Ther* 2000;16:139–45
- Gupta JK, Lilford RJ. **Assessment and management of fetal agenesis of the corpus callosum.** *Prenat Diagn* 1995;15:301–12
- Jeret J, Serur D, Wisniewski KE, et al. **Clinicopathological findings associated with agenesis of the corpus callosum.** *Brain Dev* 1987;9:255–64
- Parrish ML, Roessmann U, Levinsohn MW. **Agenesis of the corpus callosum: a study of the frequency of associated malformations.** *Ann Neurol* 1979;6:349–54
- Rapp B, Perrotin F, Marret H, et al. **Interet de l'IRM cerebrale foetale pour le diagnostic et le pronostic prenatal des agenesies du corps calleux.** *J Gynecol Obstet Biol Reprod* 2002;31:173–82
- Blum A, Andre M, Droulle P, et al. **Prenatal echographic diagnosis of corpus callosum agenesis.** *Genet Couns* 1990;1:115–26
- Pilu G, Sandri F, Perolo A, et al. **Sonography of fetal agenesis of the corpus callosum: a survey of 35 cases.** *Ultrasound Obstet Gynecol* 1993;3:318–29
- Vergani P, Ghindini A, Strobelt N, et al. **Prognostic indicators in the prenatal diagnosis of agenesis of corpus callosum.** *Am J Obstet Gynecol* 1994;170:753–58
- Shevell MI. **Clinical and diagnostic profile of agenesis of the corpus callosum.** *J Child Neurol* 2002;17:896–900
- Francesco P, Maria-Edgarda F, Giovanni P, et al. **Prenatal diagnosis of agenesis of corpus callosum: what is the neurodevelopmental outcome?** *Pediatr Int* 2006;48:298–304
- Busse R, Carrillo A, Brittain JH, et al. *On-Demand Real-Time Imaging: Interactive Multislice Acquisition Applied to Prostate and Fetal Imaging—Proceedings of the Tenth Scientific Meeting and Exhibition of International Society for Magnetic Resonance in Medicine*, Honolulu, Hawaii, 18–25 May 2002
- Garel C. *MRI of the Fetal Brain: Normal Development and Cerebral Pathologies*. Berlin, Germany: Springer-Verlag; 2004:1–267
- Garel C, Chantrel E, Brisse H, et al. **Fetal cerebral cortex: normal gestational landmarks identified using prenatal MR imaging.** *AJNR Am J Neuroradiol* 2001;22:184–89
- Pinheiro J, Bates DM. *Mixed-Effects Models in S and S-PLUS*. New York, NY: Springer-Verlag; 2000
- Hetts SW, Sherr EH, Chao S, et al. **Anomalies of the corpus callosum: an MR analysis of the phenotypic spectrum of associated malformations.** *AJR Am J Roentgenology* 2006;187:1343–48
- Van Essen D. **A tension-based theory of morphogenesis and compact wiring in the central nervous system.** *Nature* 1997;385:313–18
- Toro R, Burnod Y. **A morphogenetic model for the development of cortical convolutions.** *Cereb Cortex* 2005;15:1900–13. Epub 2005 Mar 9
- Hilgetag CC, Barbas H. **Developmental mechanics of the primate cerebral cortex.** *Anat Embryol (Berl)* 2005;210:411–17
- Fischl B, Rajendran N, Busa E, et al. **Cortical folding patterns and predicting cytoarchitecture.** *Cereb Cortex* 2008;18:1973–80. Epub 2007 Dec 12
- Lee S, Mori S, Kim DJ, et al. **Diffusion tensor MR imaging visualizes the altered hemispheric fiber connection in callosal dysgenesis.** *AJNR Am J Neuroradiol* 2004;25:25–28
- Tovar-Moll F, Moll J, de Oliveira-Souza R, et al. **Neuroplasticity in human callosal dysgenesis: a diffusion tensor imaging study.** *Cereb Cortex* 2007;17:531–41. Epub 2006 Apr 20
- Utsunomiya H, Yamashita S, Takano K, et al. **Arrangement of fiber tracts forming Probst bundle in complete callosal agenesis: report of two cases with an evaluation by diffusion tensor tractography.** *Acta Radiol* 2006;47:1063–66
- d'Ercole C, Girard N, Cravello L, et al. **Prenatal diagnosis of fetal corpus callosum agenesis by ultrasonography and magnetic resonance imaging.** *Prenat Diagn* 1998;18:247–53
- Fratelli N, Papageorhiou AT, Prefumo F, et al. **Outcome of prenatally diagnosed agenesis of the corpus callosum.** *Prenat Diagn* 2007;27:512–17
- Sonigo PC, Rypeno FF, Carteret M, et al. **MR imaging of fetal cerebral anomalies.** *Pediatr Radiol* 1998;28:212–22
- Bedeschi MF, Bonaglia MC, Grasso R, et al. **Agenesis of the corpus callosum: clinical and genetic study in 63 young patients.** *Pediatr Neurol* 2006;34:186–93
- Garel C, Brisse H, Elmaleh M, et al. **Magnetic resonance imaging of the fetus.** *Pediatr Radiol* 1998;28:201–11
- Levine D, Barnes PD, Madsen JR, et al. **Fetal central nervous system anomalies: MR imaging augments sonographic diagnosis.** *Radiology* 1997;204:635–42
- Moutard ML, Keiffer V, Feingold J, et al. **Agenesis of corpus callosum: prenatal diagnosis and prognosis.** *Childs Nerv Syst* 2003;19:471–76. Epub 2003 Jul 4
- Chadie A, Radi S, Trestart L, et al. **Neurodevelopmental outcome in prenatally diagnosed isolated agenesis of the corpus callosum.** *Acta Paediatr* 2008;97:420–24. Epub 2008 Feb 27